# Synthesis, Characterization, Anti-mycobacterial evaluation, In-Vitro and Computational analysis of Pyrazole derivative

**Deepa Deependra Gupta[a*], V. J. Desale[b], B. R. Thorat[c], R.S. Yamgar[d]**

[a] P.G. and Research Centre, Department of Chemistry, Government of Maharashtra's Ismail Yusuf College, Jogeshwari, Mumbai-400060, India.

[b] Department of Chemistry, HPT Arts and RYK Science College, Nashik-05

[c] Department of Chemistry, Government College of Arts and Science, Chhatrapati Sambhajinagar

[d] Department of Chemistry, Patkar-Varde College of Arts, Science and Commerce, Goregaon, Mumbai

**ABSTRACT**

Pyrazole derivatives have gained considerable interest in medicinal chemistry due to their diverse pharmacological properties, including antituberculosis activity. This study focuses on the synthesis, characterization, ADMET-SAR predictions, and biological evaluation of substituted pyrazole derivatives of 3-(4-methoxyphenyl)-3-oxopropanoate.) The synthesized compounds were characterized using spectral techniques, including NMR, IR, and mass spectroscopy. ADMET-SAR analysis predicted the pharmacokinetics and drug-likeness of these compounds, and their antituberculosis activity was evaluated against *Mycobacterium tuberculosis* strains. The results indicated promising biological activity and favourable drug-like properties, suggesting their potential as lead molecules for the development of antituberculosis drugs.

**KEYWORDS**

Pyrazole, Hydrazides, antituberculosis, ADMET-SAR, drug design, pharmacokinetics.

## INTRODUCTION

Tuberculosis (TB), caused by *Mycobacterium tuberculosis*, remains a global health challenge.[1-3] The emergence of multidrug-resistant (MDR) and extensively drug-resistant (XDR) strains necessitates the discovery of novel therapeutic agents[4]. Pyrazole derivatives have emerged as promising scaffolds due to their diverse biological activities, including antituberculosis properties[5-8]. This study explores the synthesis and biological evaluation of pyrazole derivatives of 3-(4-methoxyphenyl)-3-oxopropanoate, a chemical scaffold with potential antituberculosis activity. Various pyrazole derivatives containing quinoline, furan, indole, pyridine, pyrimidine, coumarin, purine, pyrrole, benzofuran, benzoxazoles, etc, are reported in the literature showing anti-tuberculosis activity[9].

Tuberculosis (TB) remains one of the deadliest infectious diseases worldwide, with an estimated 10 million cases and 1.5 million deaths annually, according to the World Health Organization (WHO)[10-11]. Despite significant advancements in medical science, TB continues to pose a global health threat, particularly in developing and underdeveloped nations. One of

the critical challenges in combating TB is the emergence of multidrug-resistant (MDR) and extensively drug-resistant (XDR) strains of *Mycobacterium tuberculosis*. These strains have rendered many first-line and second-line TB drugs ineffective, necessitating the urgent development of novel therapeutic agents [12-15].

Pyrazole is a five-membered heterocyclic compound containing two adjacent nitrogen atoms in its ring structure. The pyrazole scaffold has attracted substantial attention in medicinal chemistry due to its versatility and broad spectrum of biological activities. As a five-membered heterocyclic compound containing two nitrogen atoms, pyrazole derivatives have demonstrated diverse pharmacological properties, including anticancer, anti-inflammatory, antimalarial, and antituberculosis activities [16- 20]. In particular, the structural adaptability of pyrazole derivatives enables extensive modifications, thereby enhancing their interactions with specific biological targets. It is very important to note that studies published by Desale et al (2019), Haroon ur Rashid et al, Diego G. Ghiano et al, and Rafal M. Mohareb, et al. have shown very peculiar anti-tubercular activities [1.5- 12.5 µg/ml][21-24].

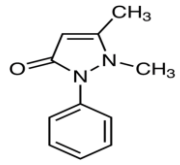
Anti-pyrine

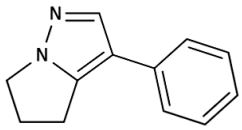
Wthasomnine

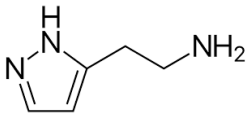
Betazole

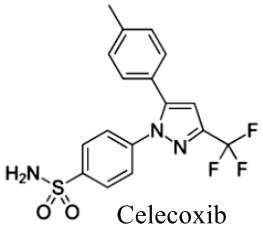
Celecoxib

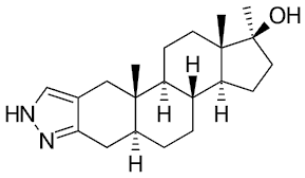
Stanozolol

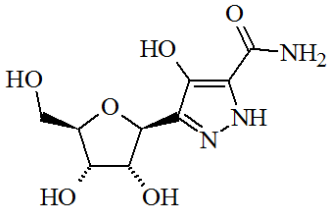
Pyrazofurin

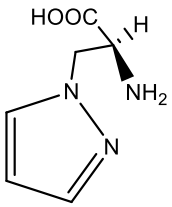
2-amino-3-(pyrazolyl)propanoic acid

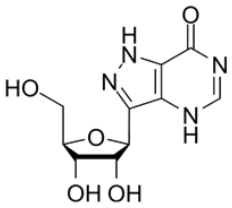
Formycin

**Natural Products and Drugs Containing Pyrazole Moieties[25]:**

Among the pyrazole derivatives, 3-(4-methoxyphenyl)-3-oxopropanoate is a promising precursor, offering unique structural features suitable for antituberculosis drug design. The incorporation of functional groups into this scaffold can improve its pharmacokinetic properties, including absorption, distribution, metabolism, excretion, and toxicity (ADMET). Advances in computational techniques, such as ADMET-SAR (Structure-Activity Relationship) modelling, have enabled researchers to predict the pharmacokinetic and toxicological profiles of drug candidates, accelerating the drug discovery process [26- 30.]

This study aims to synthesize and characterize substituted pyrazole derivatives of 3-(4-methoxyphenyl)-3-oxopropanoate and evaluate their antituberculosis potential. The synthesis of novel compounds involves optimizing reaction conditions to ensure high yields and purity. Characterization techniques such as nuclear magnetic resonance (NMR), infrared (IR) spectroscopy, and mass spectrometry are employed to confirm the molecular structures of the synthesized compounds.

Furthermore, the study leverages ADMET-SAR analysis to predict the pharmacological profiles of the compounds, ensuring their compatibility with drug-like properties. The synthesized compounds are then tested against *Mycobacterium tuberculosis* strains to assess their biological activity. This dual approach of computational and experimental evaluation offers a comprehensive understanding of the compounds' potential as antituberculosis agents. By minimizing the use of hazardous reagents and optimizing reaction conditions, the study not only contributes to the discovery of new TB drugs but also promotes environmentally friendly research methodologies.

## MATERIAL AND METHODS:

All chemicals and solvents were procured from Merck chemicals and further purified them whenever necessary. The Thin layer chromatographic technique (TLC 0.25 mm E-Merck silica gel 60 F254 pre-coated plates) was implemented to conduct all necessary reactions. TLC plates after spotting were further visualised with UV light. All compounds were tested for their respective melting points using apparatus from Sunder Industrial Products, Mumbai, and they were all uncorrected. We have recorded $^{1}$H-NMR spectra on a 300 MHz Agilent instrument. The FT–IR spectral analysis was carried out by using the Perkin Elmer Tensor-II model [31- 32.]

## SYNTHESIS OF PYRAZOLES:

**Synthesis of different pyrazoles derivatives(3a-3j):** Pyrazoles derivatives were synthesized from substituted aryl hydrazide(**1a-j**) and ethyl 3-(4-methoxyphenyl)-3-Oxoproanoate (**2**)

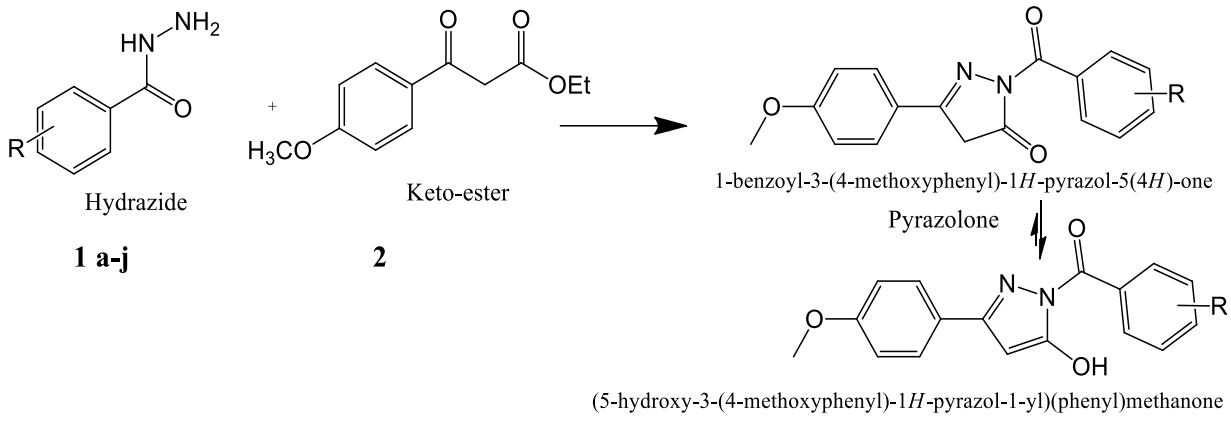


Add an equimolar quantity of 1,3-diketones/ketoesters and acyl hydrazide into absolute ethanol containing a catalytic amount of acetic acid, and reflux the reaction mixture till completion of the reaction in a water bath. The reaction takes 1-4 hrs to complete. Monitor the progress of the reaction by performing TLC time to time in ethyl acetate -pet ether (1:9) as the mobile phase. After completion of the reaction, distil out the solvent and cool it to room temperature stir for a few minutes. The solid product formed was filtered, washed with water and cold ethanol, dried, and then crystallized from ethanol.

**TABLE 1: Experimental parameters and melting point of different synthesised pyrazole Derivatives**

| Hydrazides: 1a-1j | Pyrazole derivatives: 3a-3j | Yield (%) | Colour | m.p. (°C) |
|---|---|---|---|---|
| 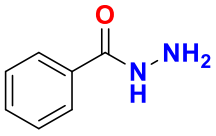 1a | 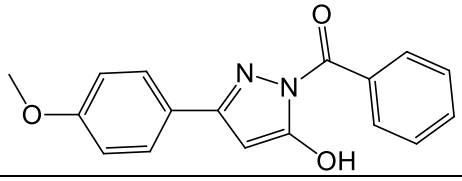 | 68 | Buff white | 190 |
| 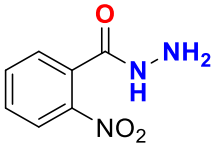 1b | 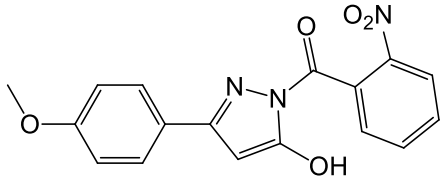 | 70 | white | 180 |
| 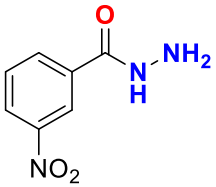 1c | 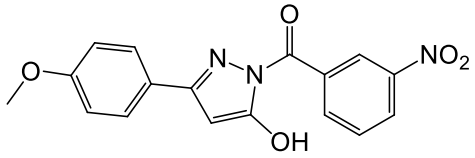 | 63 | Buff white | 204 |
| 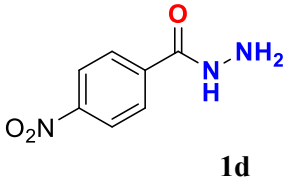 1d | 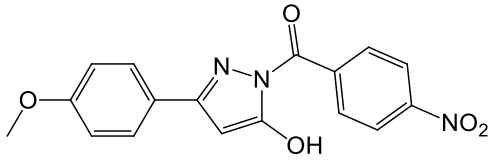 | 60 | Buff white | 152 |

| | | | | |
|---|---|---|---|---|
| 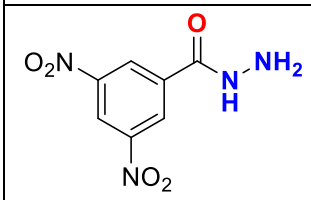 1e | 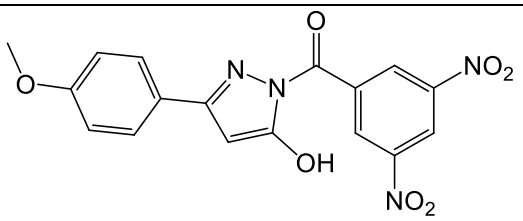 | 65 | Light Yellow | 240 |
| 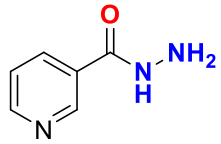 1f | 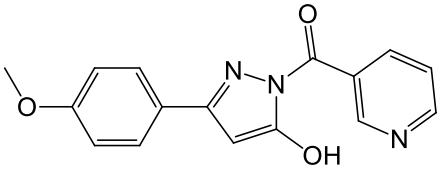 | 61 | Buff white | 180 |
| 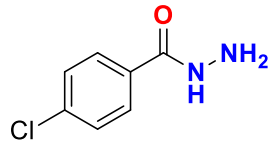 1g | 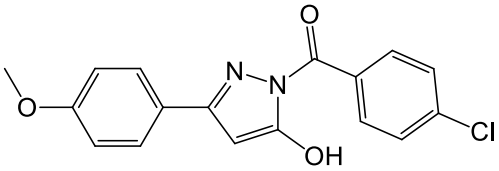 | 66 | Buff white | 272 |
| 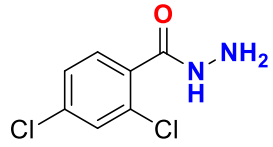 1h | 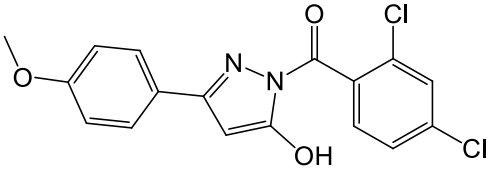 | 72 | Buff white | 160 |
| 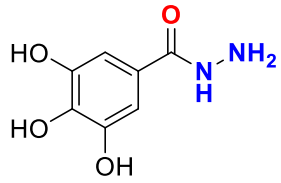 | 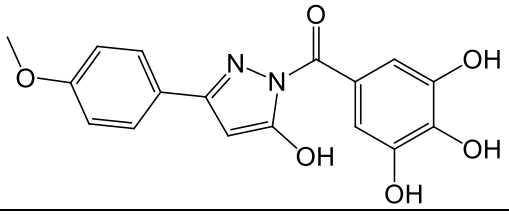 | 62 | Buff white | 220 |
| 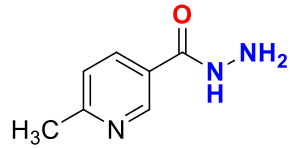 1j | 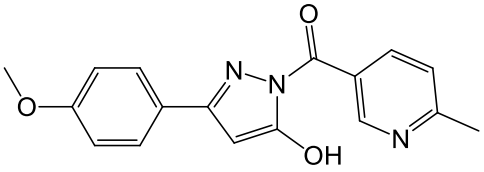 | 68 | Buff white | 320 |

**TABLE 2: Spectral characterization of synthesised hydrazones (3a-3j)**

| Pyrazole derivatives | FT- IR data ($cm^{-1}$) | | | | $^1$HNMR chemical shifts of proton in δ | | |
|---|---|---|---|---|---|---|---|
| | Enolic-OH | >N-C=O | Ar-O - | C-O-C Stretching | Enolic-OH | > N-C=CH | O-$CH_3$ |
| 3a | 3200 | 1666 | 1250 | 1029 | 10.34 | 5.75 | 3.82 |
| 3b | 3162 | 1635 | 1250 | 1029 | 10.95 | 5.71 | 3.81 |
| 3c | 3601 | 1667 | 1251 | 1029 | 11.05 | 5.70 | 3.82 |
| 3d | 3698 | 1670 | 1277 | 1030 | 10.98 | 5.72 | 3.81 |

| | | | | | | | |
|---|---|---|---|---|---|---|---|
| 3e | 3303 | 1608 | 1270 | 1031 | 11.69 | 5.73 | 3.81 |
| 3f | 3698 | 1678 | 1251 | 1029 | 10.81 | 5.73 | 3.81 |
| 3g | 3697 | 1681 | 1249 | 1029 | 10.61 | 5.52 | 3.81 |
| 3h | 3123 | 1697 | 1250 | 1028 | 11.65 | 5.72 | 3.80 |
| 3i | 3292 | 1670 | 1249 | 1028 | 11.65 | 5.72 | 3.79 |
| 3j | 3698 | 1593 | 1250 | 1028 | 11.65 | 5.71 | 3.80 |

**EXPERIMENTAL DATA:**

**1. (5-hydroxy-3-(4-methoxyphenyl)-1H-pyrazol-1-yl) (phenyl) methanone (3a)**

Yield (%): 68; m.p. ($^0$C): 190.

FT-IR (cm$^{-1}$): 3200, 3000.67, 2836,31, 1666, 1628, 1618, 1532, 1577, 1487, 1445, 1286.15, 1249.94, 1068, 1029.8, 869, 836, 795.

$^1$HNMR (300 MHz, $D_6$ DMSO) δ ppm): 3.82 (s) 3H, 5.75 d (s) 1H, 6.91 (d, J:8.7Hz) 2H, 7.99 (d, J:7.5Hz) 2H, 7.47 (t, J:7.5Hz) 2H, 7.55 (t, J:8.7Hz) 3H, 10.34 (s) 1H.

Elemental analysis Calculated for: $C_{17}H_{14}N_2O_3$ found C, 69.38; H, 4.79; N, 9.52; O, 16.37.

m/Z: 294.10

**2. (5-hydroxy-3-(4-methoxyphenyl)-1H-pyrazol-1-yl) (2-nitrophenyl) methanone (3b)**

Yield (%):70; m.p. ($^0$C): 180.

FT-IR (cm-1): 3162, 3012, 2837, 1598, 1580, 1573, 1531, 1498, 1485, 1442, 1250, 1029, 836, 761, 660.

$^1$H-NMR (δ in ppm, 300 MHz, $D_6$ DMSO): 3.81 (s) 3H,5.71 (s) 1H, 6.90 (d, J:8.7Hz) 2H, 7.56 (d, J:8.7Hz) 2H, 7.69 (m) 2H, 8.07 (d, J:8.1Hz) 2H, 10.95 (s) 1H.

Elemental analysis Calculated for: $C_{17}H_{13}N_3O_5$ found C, 60.18; H, 3.86; N, 12.38; O, 23.58.

m/Z: 339.09

**3. (5-hydroxy-3-(4-methoxyphenyl)-1H-pyrazol-1-yl) (3-nitrophenyl) methanone (3c)**

Yield (%): 63; m.p. ($^0$C): 204.

FT-IR (cm-1): 3601, 3073, 2849, 1667, 1608, 1573, 1531, 1351, 1251, 1029, 835, 772, 726, 658.

$^1$H-NMR (δ in ppm, 300 MHz, $D_6$ DMSO): 3.82 (s) 3H, 5.7 (s) 1H, 6.91 (d, J:9.0 Hz) 2H, 7.71 (d, J:7.5 Hz) 2H, 7.75 (m, J:7.5 Hz) 2H, 8.41 (s) 1H, 8.96 (s) 1H, 11.05 (s) 1H.

Elemental analysis Calculated for: $C_{17}H_{13}N_3O_5$ found C, 60.18; H, 3.86; N, 12.38; O, 23.58.

m/Z: 339.09

**4. (5-hydroxy-3-(4-methoxyphenyl)-1H-pyrazol-1-yl) (4-nitrophenyl) methanone (3d)**

Yield (%): 60; m.p. ($^0$C): 152.

FT-IR (cm-1): 3698, 3169, 2840,1580, 1514,1445, 1470, 1298, 1277, 1177, 838, 790, 710.

$^1$H-NMR (δ in ppm, 300 MHz, $D_6$ DMSO): 3.81 (s) 3H, 5.72 (s) 1H, 6.90 (d, J:6.9 Hz) 2H, 7.56 (d, J:6.9 Hz) 2H, 7.87 (d, 7.2Hz) 2H, 8.24 (d, J:7.2Hz) 2H, 10.98 (s) 1H.
Elemental analysis Calculated for: $C_{17}H_{13}N_3O_5$ found C, 60.18; H, 3.86; N, 12.38; O, 23.58.
m/Z: 339.09

**5. (3,5-dinitrophenyl) (5-hydroxy-3-(4-methoxyphenyl)-1H-pyrazol-1-yl) methanone (3e)**

Yield (%): 65; m.p. ($^0$C): 240.
FT-IR (cm-1): 3303, 3214, 3106, 2979, 1608, 1583, 1542.47, 1520, 1495, 1485,1440, 1323,1270, 1257, 1178, 1031, 837, 816, 730, 653.
$^1$H-NMR (δ in ppm, 300 MHz, $D_6$ DMSO): 3.81 (s) 3H, 5.73 (s) 1H, 6.9 d (d) 2H, 7.56 (d) 2H, 9.16 (s) 1H, 9.35 (s) 2H, 11.69 (s) 1H.
Elemental analysis Calculated for: $C_{17}H_{12}N_4O_7$ found C, 58.13; H, 3.15; N, 14.58; O, 29.14; m/Z: 384.07

**6. (5-hydroxy-3-(4-methoxyphenyl)-1H-pyrazol-1-yl) (pyridin-3-yl) methanone (3f)**

Yield (%): 61; m.p. ($^0$C): 180.
FT-IR (cm-1): 3698, 3383.64, 3196.90, 2980, 1678, 1651, 1594.71, 1542, 1476, 1251, 1029, 837, 773, 697.
1H-NMR (δ in ppm, 300 MHz, $D_6$ DMSO): 3.81 (s) 3H, 5.73 (s) 1H, 6.9 (d) 2H, 7.55 (d) 2H, 7.93 (s, J: 6.6Hz), 1H, 8.30 (s), 1H, 8.75 (s) 1H, 9.17 (s) 1H, 10.81 (s) 1H.
Elemental analysis Calculated for: $C_{16}H_{13}N_3O_3$ found C, 65.08; H, 4.44; N, 14.23; O, 16.25; m/Z: 295.10.

**7. (4-chlorophenyl)(5-hydroxy-3-(4-methoxyphenyl)-1H-pyrazol-1-yl)methanone (3g)**

Yield (%): 66; m.p. ($^0$C): 272.
FT-IR (cm-1): 3697, 3168, 2980, 2865, 1681, 1639, 1589, 1561, 1437, 1296, 1249, 1175, 1063, 1029, 1010, 079, 835, 680.
1H-NMR (δ in ppm, 300 MHz, $D_6$ DMSO): 3.81 (s) 3H, 5.52 (s) 1H, 6.92 (s, J:7.5Hz) 2H, 7.56 (d, J:7.5Hz) 2H, 7.97 (d, J:7.2Hz) 2H, 8.15(d) 2H, 10.61 (s) 1H.
Elemental analysis Calculated for: $C_{17}H_{13}ClN_2O_3$ found C, 62.11; H, 3.99; N, 13.58; O, 14.60.
m/Z: 328.06

**8. (2,4-dichlorophenyl)(5-hydroxy-3-(4-methoxyphenyl)-1H-pyrazol-1-yl) methanone (3h)**

Yield (%): 72; m.p. ($^0$C): 160.
FT-IR (cm-1): 3123, 2959, 2836, 1697, 1616, 1582, 1492, 1474, 1297, 1250, 1028, 817, 743, 678.
1H-NMR (δ in ppm, 300 MHz, $D_6$ DMSO): 3.80 (s) 3H, 5.72 (s) 1H, 6.91 (d, J:8.1Hz) 2H, 7.44 (d) 2H, 7.56 (m, J:8.1Hz) 2H, 8.10 (s) 1H, 11.65 (s)1H.
Elemental analysis Calculated for: $C_{17}H_{12}Cl_2N_2O_3$ found C, 56.22; H, 3.33; N, 8.52; O, 13.22.
m/Z: 362.02

**9. (5-hydroxy-3-(4-methoxyphenyl)-1H-pyrazol-1-yl)(3,4,5-trihydroxyphenyl) methanone (3i)**

Yield (%): 62; m.p. ($^0$C): 220.

FT-IR (cm-1): 3292, 2980, 1670, 1599, 1249, 1028, 817, 743, 678;

1H-NMR (δ in ppm, 300 MHz, $D_6$ DMSO): 3.79 (s) 3H, 5.72 (s) 1H, 6.91 (d) 2H, 7.56 (d) 2H, 7.81 (s) 2H, 9.91 (s) 3H, 11.65 (s) 1H.

Elemental analysis Calculated for: $C_{17}H_{14}N_2O_6$ found C, 59.65; H, 4.12; N, 8.18; O, 28.05.

m/Z: 342.09

**10. (5-hydroxy-3-(4-methoxyphenyl)-1H-pyrazol-1-yl)(6-methylpyridin-3-yl) methanone(3j)**

Yield (%): 68; m.p. ($^0$C): 320.

FT-IR (cm-1): 3698, 2923, 2853, 1583, 1473, 1428, 1410, 1250, 1175, 1028, 794, 675;

1H-NMR (δ in ppm, 300 MHz, $D_6$ DMSO): 1.25 (s) 3H, 3.80 (s) 3H, 5.71 (s) 1H, 6.91 (d) 2H, 7.56 (d) 2H, 8.06 (m) 3H, 11.65 (s) 1H.

Elemental analysis Calculated for: $C_{17}H_{15}N_3O_3$ found C, 67.01; H, 4.89; N, 13.58; O, 15.52.

m/Z: 309.11

## RESULT AND DISCUSSION:

**$^1$H-NMR, FT-IR Spectral characterization:** The pyrazoles synthesized showed medium absorption between 3600-3200 $cm^{-1,}$ which is absent in the parent molecule, depicting an enol -OH group. In a molecule. Further absorption of the amide carbonyl group (pyrazoles) of the amide group. in the region 1660-1600 $cm^{-1}$(medium to strong) and at 1420 cm due to C=N stretching confirmed the formation of the pyrazoles ring. Further, all newly synthesized pyrazole derivative molecules have a medium absorption pattern at 1340-1100 $cm^{-1}$ due to bending vibration and at 1307-1246 $cm^{-1}$ due to stretching vibration of the C-N bond. All the compounds showed an absorption band in the region of 1250-1150 $cm^{-1}$ due to asymmetrical stretching and at 1020-1075 due to symmetrical stretching, confirming the ethereal linkage(C-O-C) in them.

The peak in the $^1$HNMR due to the -$CH_2$-CO- proton in the region of 3.7 to 4.2 ppm is absent, indicating the formation of an enolic form, which is confirmed by a peak showing a weak singlet in the deshielded area at 10-11 ppm. The data of chemical shift of >N-C=CH of newly synthesized pyrazole molecules 3a-j are summarized in Table 5. The prominent singlet at 3.79-3.81 ppm occurred due to the presence of the etherical proton of $CH_3$-O in all newly synthesized pyrazole derivatives in the deshielded zone.

We synthesized all ten pyrazoles for the sake of an efficient and cost-effective anti-tuberculosis agent and the biological importance of pyrazoles.

## STUDY OF IN VITRO ANTI-MYCOBACTERIUM TUBERCULOSIS ACTIVITY:

Mycobacteria strain used for the in vitro anti-mycobacterial tuberculosis (vaccine strain, H37RV strain): ATCC no. 27294. The anti-Tuberculosis study was performed by using the popular Microplate Alamar blue assay (MABA), as it is one of the best methods for analysis [33]. We added 200 µL of sterile deionised water into 96 perimeter wells of a sterile plate in order to minimise the evaporation of test medium in the wells during incubation. All the wells received 100 µL of the middle broth 7H9 and were allowed to be serially diluted with the test compound directly on plates. The test compounds' concentration varied from 100 to 0.2 µg/mL. All the plates were covered and sealed with parafilm and incubated at 37 $^0$C for 5 days. After that, 25 µL of freshly prepared 1:1 mixture of Alamar blue reagent and 10% Tween 80 was added to each plate and incubated further for 24 hours. Blue colour in the well was interpreted as no bacterial growth, and pink colour was treated as bacterial growth. We recorded MIC (lowest drug concentration that prevented colour changes from blue to pink) values with reference to three anti-TB drugs, namely Pyrazinamide, ciprofloxacin, and streptomycin. All the results of newly synthesised compounds are in Table 4.

All the newly synthesized hydrazones (3a-3j) showed good to moderate in vitro anti-tuberculosis activity as tested with the Microplate Alamar Blue assay (MABA) against Mycobacterium tuberculosis (vaccine strain, H37RV strain) (34). Compounds 3b MIC value: 12.5 µg/mL) and 3a is 25 µg/mL) were found to be the active compounds (Pyrazinamide and ciprofloxacin, MIC value: 3.125 µg/mL). 3c-j showed moderate MIC values of 50 µg/mL. It is worth noting that, after some structural modifications, these candidates may become promising anti-TB drug candidates in the future.

**Table 3: Minimum Inhibitory Concentration Values for Compounds (3a-3j) against H37rv Strain**

| Test samples | **3a** | **3b** | **3c** | **3d** | **3e** | **3f** | **3g** | **3h** | **3i** | **3j** | Pyr. | cipro | Strepto |
|---|---|---|---|---|---|---|---|---|---|---|---|---|---|
| MIC value (µg/mL) | 25 | 12.5 | 50 | 50 | 50 | 50 | 50 | 50 | 50 | 50 | 3.125 | 3.125 | 6.250 |

**Table 4: Probable Values of In-Silico ADMET Properties of 3a-3j molecules using AdmetSAR 3.0**

| Description/ Properties | **Probable value of Pyrazole derivatives** | | | | | | | | | |
|---|---|---|---|---|---|---|---|---|---|---|
| | **3a** | **3b** | **3c** | **3d** | **3e** | **3f** | **3g** | **3h** | **3i** | **3j** |
| Molecular weight | 294.31 | 339.30 | 339.30 | 339.30 | 384.30 | 295.29 | 328.75 | 363.2 | 342.30 | 309.32 |
| A log P | 3.368 | 3.17 | 3.134 | 3.149 | 3.104 | 1.819 | 3.939 | 4.893 | 1.62 | 2.571 |

| | | | | | | | | | | |
|---|---|---|---|---|---|---|---|---|---|---|
| H-bond Acceptor | 5 | 7 | 7 | 7 | 9 | 6 | 5 | 5 | 8 | 6 |
| H-bond Donor | 1 | 1 | 1 | 1 | 1 | 1 | 1 | 1 | 4 | 1 |
| Rotatable Bonds | 3 | 4 | 4 | 4 | 5 | 3 | 3 | 3 | 3 | 3 |
| Human intestinal absorption (HIA) | 0.947 | 0.958 | 0.961 | 0.951 | 0.938 | 0.988 | 0.972 | 0.972 | 0.652 | 0.984 |
| Caco-2 | 0.607 | 0.374 | 0.464 | 0.348 | 0.361 | 0.957 | 0.767 | 0.741 | 0.052 | 0.887 |
| Blood brain barrier (BBB) | 0.617 | 0.711 | 0.574 | 0.475 | 0.446 | 0.886 | 0.712 | 0.784 | 0.113 | 0.87 |
| OATP2B1 inhibitor | 0.362 | 0.446 | 0.459 | 0.458 | 0.526 | 0.103 | 0.393 | 0.486 | 0.517 | 0.205 |
| OATP1B1 inhibitor | 0.893 | 0.832 | 0.793 | 0.736 | 0.7 | 0.968 | 0.85 | 0.814 | 0.798 | 0.939 |
| OATP1B3 inhibitor | 0.893 | 0.788 | 0.783 | 0.742 | 0.682 | 0.982 | 0.862 | 0.799 | 0.782 | 0.955 |
| MATE1 inhibitor | 0.222 | 0.252 | 0.246 | 0.246 | 0.275 | 0.12 | 0.207 | 0.239 | 0.253 | 0.159 |
| OCT2 inhibitor | 0.16 | 0.175 | 0.157 | 0.158 | 0.191 | 0.308 | 0.159 | 0.192 | 0.244 | 0.293 |
| BSEP inhibitor | 0.759 | 0.933 | 0.909 | 0.922 | 0.904 | 0.644 | 0.904 | 0.949 | 0.345 | 0.838 |
| P-glycoprotein inhibitor | 0.439 | 0.821 | 0.816 | 0.814 | 0.886 | 0.307 | 0.640 | 0.760 | 0.217 | 0.667 |
| P-glycoprotein substrate | 0.09 | 0.135 | 0.139 | 0.215 | 0.157 | 0.314 | 0.075 | 0.084 | 0.298 | 0.531 |
| CYP3A4 substrate | 0.283 | 0.68 | 0.606 | 0.724 | 0.673 | 0.467 | 0.574 | 0.774 | 0.056 | 0.878 |
| CYP2C9 substrate | 0.342 | 0.687 | 0.672 | 0.721 | 0.703 | 0.463 | 0.638 | 0.766 | 0.036 | 0.755 |
| CYP2D6 substrate | 0.183 | 0.253 | 0.244 | 0.317 | 0.245 | 0.263 | 0.249 | 0.328 | 0.022 | 0.577 |
| CYP3A4 inhibition | 0.333 | 0.813 | 0.705 | 0.607 | 0.703 | 0.462 | 0.447 | 0.494 | 0.170 | 0.238 |
| CYP2C9 inhibition | 0.831 | 0.943 | 0.897 | 0.843 | 0.88 | 0.745 | 0.897 | 0.919 | 0.407 | 0.576 |
| CYP2D6 inhibition | 0.095 | 0.126 | 0.104 | 0.082 | 0.156 | 0.24 | 0.126 | 0.174 | 0.226 | 0.134 |
| CYP1A2 inhibition | 0.795 | 0.699 | 0.694 | 0.314 | 0.663 | 0.806 | 0.799 | 0.833 | 0.803 | 0.626 |
| Rodent Carcinogenicity | 0.335 | 0.408 | 0.502 | 0.468 | 0.547 | 0.432 | 0.368 | 0.332 | 0.474 | 0.396 |
| Eye corrosion | 0.245 | 0.027 | 0.035 | 0.013 | 0.037 | 0.002 | 0.186 | 0.165 | 0.092 | 0.001 |
| Eye irritation | 0.96 | 0.486 | 0.57 | 0.19 | 0.467 | 0.03 | 0.903 | 0.858 | 0.902 | 0.024 |
| Ames mutagenesis | 0.326 | 0.716 | 0.852 | 0.792 | 0.893 | 0.276 | 0.492 | 0.47 | 0.264 | 0.471 |
| Human either-a-go-go inhibition (10-30 uM) | 0.374 | 0.772 | 0.807 | 0.753 | 0.866 | 0.239 | 0.757 | 0.909 | 0.549 | 0.796 |
| Micronuclear | 0.509 | 0.849 | 0.822 | 0.857 | 0.832 | 0.827 | 0.614 | 0.6 | 0.409 | 0.882 |
| Nephrotoxicity | 0.502 | 0.534 | 0.644 | 0.534 | 0.641 | 0.393 | 0.598 | 0.57 | 0.424 | 0.381 |
| Respiratory toxicity | 0.078 | 0.29 | 0.213 | 0.449 | 0.365 | 0.917 | 0.097 | 0.0093 | 0.409 | 0.82 |
| Acute Oral Toxicity (c) | 0.591 | 0.466 | 0.499 | 0.666 | 0.443 | 0.824 | 0.673 | 0.52 | 0.094 | 0.765 |
| Estrogen receptor binding | 0.346 | 0.358 | 0.448 | 0.453 | 0.425 | 0.059 | 0.541 | 0.677 | 0.401 | 0.22 |
| Androgen receptor binding | 0.297 | 0.523 | 0.501 | 0.479 | 0.509 | 0.114 | 0.418 | 0.5 | 0.315 | 0.349 |
| Thyroid receptor binding | 0.193 | 0.287 | 0.373 | 0.334 | 0.383 | 0.117 | 0.412 | 0.587 | 0.167 | 0.244 |

| | | | | | | | | | | |
|---|---|---|---|---|---|---|---|---|---|---|
| Glucocorticoid receptor binding | 0.227 | 0.45 | 0.468 | 0.498 | 0.529 | 0.152 | 0.423 | 0.574 | 0.237 | 0.308 |
| Aromatase binding | 0.474 | 0.452 | 0.441 | 0.347 | 0.395 | 0.419 | 0.532 | 0.526 | 0.392 | 0.46 |
| Honey bee toxicity | 0.073 | 0.059 | 0.035 | 0.052 | 0.046 | 0.045 | 0.065 | 0.109 | 0.032 | 0.033 |
| Biodegradation | 0.098 | 0.037 | 0.025 | 0.017 | 0.41 | 0.56 | 0.025 | 0.023 | 0.266 | 0.036 |
| Crustacea aquatic toxicity | 0.527 | 0.652 | 0.537 | 0.518 | 0.563 | 0.173 | 0.728 | 0.871 | 0.165 | 0.209 |
| Fish aquatic toxicity | 0.736 | 0.754 | 0.709 | 0.658 | 0.711 | 0.327 | 0.638 | 0.903 | 0.38 | 0.349 |
| Water solubility (log S) | -3.854 | -5.106 | -4.963 | -5.026 | -4.977 | -3.354 | -4.565 | -5.603 | -3.252 | -4.455 |
| Plasma protein binding (100%) | 0.978 | 0.988 | 0.939 | 0.937 | 0.9 | 0.821 | 0.996 | 0.971 | 0.11 | 0.953 |

**TABLE 5: Chemical toxicity prediction of Pyrazole derivatives using STopTox 1.0 software**

| Mole - cule | Acute inhalation Toxicity | | Acute oral toxicity | | Acute dermal Toxicity | | Eye irritation & Corrosion | | Skin sensitization | | Skin irritation & Corrosion | |
|---|---|---|---|---|---|---|---|---|---|---|---|---|
| | Predi ction | Confi dence | Predi ction | Confi dence | Predi ction | Confi dence | Predi-ction | Confi-dence | Predi ction | Confi dence | Predi ction | Confi dence |
| 3a | Non Toxic | 65 | Toxic | 58 | Non Toxic | 74 | Toxic | 78 | Non-Sensitizer | 70 | Negative | 90 |
| 3b | Non Toxic | 66 | Non-Toxic | 51 | Non Toxic | 63 | Toxic | 79 | Non sensitizer | 60 | Negative | 90 |
| 3c | Non Toxic | 66 | Toxic | 51 | Non toxic | 63 | Toxic | 79 | Non Sensitizer | 60 | Negative | 90 |
| 3d | Non toxic | 66 | Toxic | 51 | Non toxic | 63 | Toxic | 79 | Non Sensitizer | 60 | Negative | 90 |
| 3e | Non Toxic | 66 | Toxic | 51 | Non Toxic | 63 | Toxic | 79 | Non Sensitizer | 60 | Negative | 90 |
| 3f | Non Toxic | 65 | Toxic | 59 | Non toxic | 75 | Toxic | 78 | Non Sensitizer | 70 | Negative | 90 |
| 3g | Non Toxic | 66 | Toxic | 58 | Non toxic | 75 | Toxic | 76 | Non sensitizer | 70 | Negative | 80 |
| 3h | Non Toxic | 66 | Toxic | 58 | Non toxic | 75 | Toxic | 76 | Non sensitizer | 60 | Negative | 70 |
| 3i | Non Toxic | 73 | Non Toxic | 66 | Non Toxic | 78 | Toxic | 76 | Non sensitizer | 60 | Negative | 80 |
| 3j | Non Toxic | 78 | Toxic | 58 | Non Toxic | 77 | Toxic | 83 | Non Sensitizer | 70 | Negative | 90 |

**TABLE 6: Drug likeness, Drug Score, Toxicity Risk, and TSPA of 3a-3j using the Osiris program.**

| | c log P | solubility | Mol wt. | Drug likeness | Drug score | TSPA |
|---|---|---|---|---|---|---|
| 3a | 3.16 | -4.9 | 294.31 | 4.07 | 0.89 | 64.35 |
| 3b | 2.24 | -5.36 | 339.31 | 3.16 | 0.90 | 110.17 |
| 3c | 2.24 | -5.36 | 339.31 | -2.33 | 0.88 | 110.17 |
| 3d | 2.24 | -5.36 | 339.31 | -8.14 | 0.86 | 110.17 |
| 3e | 1.32 | -5.82 | 384.30 | -9.99 | 0.08 | 155.99 |
| 3f | 2.16 | -4.10 | 295.30 | -5.21 | 0.93 | 77.24 |
| 3g | 3.77 | -5.64 | 328.75 | -5.46 | 0.83 | 64.35 |

| | | | | | | |
|---|---|---|---|---|---|---|
| 3h | 4.37 | 6.37 | 363.20 | 4.92 | 0.76 | 64.35 |
| 3i | 2.12 | -4.01 | 342.31 | 5.28 | 0.91 | 125.04 |
| 3j | 2.56 | -4.47 | 309.32 | 3.92 | 0.91 | 77.24 |

**IN-VITRO SILICO ADMET PREDICTIONS:**

All synthesised pyrazoles showed good drug score and drug likeness, along with good bioactivity scores. Their Admet SAR analysis suggested that there might be strong interaction with different receptors, ligands, and enzymes[34]. The result of most of the newly synthesised compounds physiochemical parameters were found to be within the range set by Lipinski's five rules. We have taken Osiris program to make a prediction of the toxicity profile (against mutagenic, tumorigenic, irritant, and reproductive effects). The outcome of all parameters indicated a low toxicity risk profile of all compounds except 3d and 3i (found to be irritant. Compounds 3f and 3j displayed high Caco-2 cell permeability with a value of 0.957 and 0.887, respectively. Similarly, it was also noted that compounds 3f and 3j might have a high tendency to cross the BBB with a probability of 0.886 and 0.870, respectively, as comes from in-silico treatment.

The potency of the molecule to inhibit the hERG-$K^+$ channel may lead to heart arrhythmia and potentially death in the primary stage of the easy drug development process. We have studied external predicative binary and multiclass models of the molecule using "Pred-hERG"[35-37]. We saw positive (blocker) response for 3e and 3h molecules, whereas all other molecules showed a negative (non-blocker) response

All new synthesised molecule shows no any activeness towards MATE, OCT2 inhibition, CYP2D6 substrate, and UGT catalysed reaction.

All newly synthesized compounds were predicted to show non-skin sensitization. Compound 3i was found to be a non-toxic molecule, and all others showed oral toxicity from the in-silico model. The human colon adenocarcinoma cell line (Caco-2) is used to design good intestinal absorption and defensive properties of the mucosa of the intestine. Each molecule showed good in silico intestinal absorption (HIA% % was> 30%). Ames mutagenesis test is used to identify by revert mutants and mutagenicity of environmental samples [38- 39.]

All our synthesised compounds did not exhibit acute inhalation toxicity and dermal toxicity against OECD TG 403,436 and OECD TG 402, respectively, as checked in silico rat models. All compounds presented inactiveness towards MATE 1, OCT2 inhibition, CYP2D6 substrate, and UGT catalysed reactions. Compounds 3a to 3j were predicted to have skin non-

sensitization. Compound 3i was found to be Non-toxic against OECD TG 401, 420, 423, and 425 of rats. All the compounds showed eye irritation and corrosion toxicity against OECD TG 405 of the rabbit. Molecules 3a and 3i showed human oral toxicity as predicted from in-silico models. The human colon adenocarcinoma cell line (Caco-2) is used to design good intestinal absorption. Ames mutagenesis test is used to identify revertant mutations and mutagenicity of environmental samples. It is also used to detect suitable mutants. Compounds (mutant) 3b,3c, 3d, and 3e were also observed to be positive in the Ames mutagenesis test. All the compounds displayed Ames's test probability within the range 0.50-0.6. All the molecules were predicted to be non-nephrotoxic. Only 3f shows respiratory toxicity. All the molecules were observed for moderate acute oral toxicity and class III toxicity as calculated from in-silico results. All the compounds were found to be in silico non-carcinogenic. Moreover, we also noticed the fact that our compounds might have a mitochondrial subcellular localization profile. Compounds 3a TO 3j did not display any honey bee toxicity and also showed fish aquatic non-toxicity, except compound 3i.

## CONCLUSION:

The synthesized pyrazole derivatives exhibited promising structural and pharmacokinetic properties. ADMET-SAR analysis indicated good absorption and low toxicity profiles, supporting their potential as drug candidates. Biological assays demonstrated moderate to good antituberculosis activity, correlating with their predicted pharmacokinetics. Compound 3b (MIC value 12.5 µg/ml) did not show any oral toxicity and was found to be most active against Mycobacterium tuberculosis (H37 RV)[40-42]. We get to know from the in-silico test, all were non-carcinogenic. However, further in vivo studies are essential to confirm efficacy and safety. Further studies, including in vivo evaluations and mechanism-of-action investigations, are recommended to advance these molecules as therapeutic candidates.

## CONFLICTS OF INTEREST

None

## ACKNOWLEDGEMENT:

The authors are thankful to the Head of the chemistry department and Principal of the college, Government of Maharashtra's Ismail Yusuf College of Arts, Science and

Commerce, Mumbai 400060, India, for providing essential research facilities and giving moral support.

**REFERENCES:**

1. Faisal M, Saeed A, Hussain S, Dar P, Larik FA. Recent developments in synthetic chemistry and biological activities of pyrazole derivatives. J Chem Sci. 2019 Aug 1;131(8).

2. Srivastava S, Kumar Rajput N, Rajendiran K, Lal Guru Jambheshwar K, Kumar N, Kanagaraj R, et al. Modeling molecular interactions of propounded pyrazole based drug candidates against bacterial DNA gyrase: Validation by syntheses and biological studies. Artic J Mol Struct [Internet]. 2019 [cited 2020 Sep 20]; Available from: https://doi.org/10.1016/j.molstruc.2019.05.125

3. Bhat MA, Al-Omar MA. Synthesis, characterization, and in vitro anti-Mycobacterium tuberculosis activity of terpene Schiff bases. Med Chem Res [Internet]. 2013 Sep 12 [cited 2020 Sep 22];22(9):4522–8. Available from: http://link.springer.com/10.1007/s00044-012-0458-3

4. Bakal RL, Gattani SG. Identification and development of 2,5-disubstituted oxadiazole as potential candidate for treatment of XDR and MDR tuberculosis. Eur J Med Chem. 2012;47(1):278–82.

5. Fustero S, María S, Barrio P, Sim A. From 2000 to Mid-2010 : A Fruitful Decade for the Synthesis of Pyrazoles. 2011;6984–7034.

6. Fahmy HH, Khalifa NM, Nossier ES, Abdalla MM, Ismai MMF. Synthesis and anti-inflammatory evaluation of new substituted 1-(3-chlorophenyl)-3-(4-methoxyphenyl)-1H-pyrazole derivatives. Acta Pol Pharm - Drug Res. 2012;69(3):411–21.

7. Khan M, Verma G, Ali I, Ali A, Chashoo G, Alam M, et al. Synthesis of pyrazole acrylic acid based oxadiazole and amide derivatives as antimalarial and anticancer agents. Bioorg Chem. 2018;77.

8. Faisal M, Saeed A, Hussain S, Dar P. Recent developments in synthetic chemistry and biological activities of pyrazole derivatives. J Chem Sci [Internet]. 2019;0123456789. Available from: https://doi.org/10.1007/s12039-019-1646-1

9. Ansari A, Ali A, Asif M, Shamsuzzaman. Review: biologically active pyrazole derivatives. New J Chem [Internet]. 2016;41(1):16–41. Available from: http://dx.doi.org/10.1039/C6NJ03181A

10. Dhamnetiya D, Patel P, Jha RP, Shri N, Singh M, Bhattacharyya K. Trends in incidence and mortality of tuberculosis in India over past three decades: a joinpoint and age–period–cohort analysis. BMC Pulm Med [Internet]. 2021;21(1):1–14. Available from: https://doi.org/10.1186/s12890-021-01740-y

11. Selvaraju S, Velayutham B, Rao R, Rade K, Thiruvengadam K, Asthana S, et al. Prevalence and factors associated with tuberculosis infection in India. J Infect Public Health [Internet]. 2023;16(12):2058–65. Available from: https://doi.org/10.1016/j.jiph.2023.10.009

12. Chatterjee S, Das P, Shikhule A, Munje R, Vassall A. Journey of the tuberculosis patients in India from onset of symptom till one-year post-treatment. PLOS Glob Public Heal [Internet]. 2023;3(2):1–19. Available from: http://dx.doi.org/10.1371/journal.pgph.0001564

13. Mandal S, Rao R, Joshi R. Estimating the Burden of Tuberculosis in India: A Modelling Study. Indian J Community Med. 2023 Jul 1;48(3):436–42.

14. Roy P, Das A, Panda A, T S, Priyadarshani A, Patro BK. India marching towards TB elimination: How far we are. Indian J Tuberc. 2024 Apr 1;71(2):213–8.

15. Prevalence and factors associated with tuberculosis infection in India - ScienceDirect [Internet]. [cited 2025 Jun 19]. Available from: https://www.sciencedirect.com/science/article/pii/S1876034123003362

16. Singh R, Kaur R, Ahlawat P, Kaushik P, Singh R, Kaur R. Green Methods for the Synthesis of Pyrazoles : A Review Green Methods for the Synthesis of Pyrazoles : A Review. Org Prep Proced Int [Internet]. 2021;53(4):317–51. Available from: https://doi.org/10.1080/00304948.2021.1904750

17. Bekhit AA, Hymete A, Asfaw H, Bekhit AEDA. Synthesis and biological evaluation of some pyrazole derivatives as anti-malarial agents. Arch Pharm (Weinheim). 2012;345(2):147–54.

18. Ahamad Syed M, Kallanagouda Ramappa A, Alegaon S. SYNTHESIS AND

EVALUATION OF ANTITUBERCULAR AND ANTI FUNGAL ACTIVITY OF SOME NOVEL 6-(4-SUBSTITUTED ARYL)-2-(3,5-DIMETHYL-1H-PYRAZOL-1-YL) IMIDAZO[2,1-B] [1,3,4] THIADIAZOLE DERIVATIVES [Internet]. Citeseer. 2013 [cited 2020 Sep 20]. Available from: http://citeseerx.ist.psu.edu/viewdoc/download?doi=10.1.1.837.4315&rep=rep1&type=pdf

19. Rochais C, Sopkovà-de Oliveira Santos J, Dallemagne P, Rault S. Synthesis of novel pyrazolopyrrolizinones as prospective anticancer agents. Heterocycles. 2006;68(10):2063–77.

20. Malvar DDC, Ferreira RT, De Castro RA, De Castro LL, Freitas ACC, Costa EA, et al. Antinociceptive, anti-inflammatory and antipyretic effects of 1.5-diphenyl-1H-Pyrazole-3-carbohydrazide, a new heterocyclic pyrazole derivative. Life Sci [Internet]. 2014;95(2):81–8. Available from: http://dx.doi.org/10.1016/j.lfs.2013.12.005

21. Desale VJ, Yamgar RS. Synthesis , Characterization , and Anti-Mycobacterial Evaluation of Oxadiazole and Pyrazolone Derivatives. 2025;14(2):1241–4.

22. Rashid H ur, Martines MAU, Duarte AP, Jorge J, Rasool S, Muhammad R, et al. Research developments in the syntheses, anti-inflammatory activities and structure-activity relationships of pyrimidines. RSC Adv. 2021;11(11):6060–98.

23. Ghiano DG, Recio-Balsells A, Bortolotti A, Defelipe LA, Turjanski A, Morbidoni HR, et al. New one-pot synthesis of anti-tuberculosis compounds inspired on isoniazid. Eur J Med Chem. 2020;208:1–15.

24. Zhao Z, Dai X, Li C, Wang X, Tian J, Feng Y, et al. Pyrazolone structural motif in medicinal chemistry: Retrospect and prospect. Eur J Med Chem [Internet]. 2020;186:111893. Available from: https://doi.org/10.1016/j.ejmech.2019.111893

25 Beyzaei, Hamid & Motraghi, Zahra & Aryan, Reza & Zahedi, Mohammad & Kermani, Alireza. (2017). Green One-pot Synthesis of Novel Polysubstituted Pyrazole Derivatives as Potential Antimicrobial Agents. Acta Chimica Slovenica. 64. 911-918. 10.17344/acsi.2017.3609.

26. Yele V, Azam MA, Wadhwani AD. Synthesis, Molecular Docking and Biological Evaluation of 2-Aryloxy-N-Phenylacetamide and N′-(2-Aryloxyoxyacetyl)

Benzohydrazide Derivatives as Potential Antibacterial Agents. Chem Biodivers. 2021;18(4).

27. Ibrahim TS, Moustafa AH, Almalki AJ, Allam RM, Althagafi A, Md S, et al. Novel chalcone/aryl carboximidamide hybrids as potent anti-inflammatory via inhibition of prostaglandin E2 and inducible NO synthase activities: design, synthesis, molecular docking studies and ADMET prediction. J Enzyme Inhib Med Chem [Internet]. 2021;36(1):1067–78. Available from: https://doi.org/10.1080/14756366.2021.1929201

28. Channar PA, Saeed A, Larik FA, Rashid S, Iqbal Q, Rozi M, et al. Design and synthesis of 2,6-di(substituted phenyl)thiazolo[3,2-b]-1,2,4-triazoles as α-glucosidase and α-amylase inhibitors, co-relative Pharmacokinetics and 3D QSAR and risk analysis. Biomed Pharmacother [Internet]. 2017;94:499–513. Available from: http://dx.doi.org/10.1016/j.biopha.2017.07.139

29. EN-NAHLI F, HAJJI H, OUABANE M, Aziz AJANA M, SEKATTE C, LAKHLIFI T, et al. ADMET profiling and molecular docking of pyrazole and pyrazolines derivatives as antimicrobial agents. Arab J Chem [Internet]. 2023;16(11):105262. Available from: https://doi.org/10.1016/j.arabjc.2023.105262

30. Bultum LE, Tolossa GB, Kim G, Kwon O, Lee D. In silico activity and ADMET profiling of phytochemicals from Ethiopian indigenous aloes using pharmacophore models. Sci Rep [Internet]. 2022;12(1):1–19. Available from: https://doi.org/10.1038/s41598-022-26446-x

31. Faïon L, Djaout K, Pintiala C, Piveteau C, Leroux F, Biela A, et al. Exploring the Antitubercular Activity of Anthranilic Acid Derivatives: From MabA (FabG1) Inhibition to Intrabacterial Acidification. Pharmaceuticals. 2023;16(3).

32. Mandewale MC, Thorat BR, Yamgar RS. Synthesis and anti-mycobacterium study of some fluorine containing schiff bases of quinoline and their metal complexes. Der Pharma Chem. 2015;7(5):207–15.

33. Maddi R, Devilal K, Babu S, Harika P. In-vitro MABA anti-tuberculosis assay of Eclipta Alba ( L .) Hassk whole plant. Pharma Innov J. 2017;6(5):103–5.

34. Abate D, Tedla Y, Meressa D, Ameni G. Isoniazid and rifampicin resistance mutations and their effect on second-line anti-tuberculosis treatment. Int J Tuberc Lung Dis.

2014;18(8):946–51.

35. Melgari D, Zhang Y, El Harchi A, Dempsey CE, Hancox JC. Molecular basis of hERG potassium channel blockade by the class Ic antiarrhythmic flecainide. J Mol Cell Cardiol [Internet]. 2015;86:42–53. Available from: http://dx.doi.org/10.1016/j.yjmcc.2015.06.021

36. Cheng H, Zhang Y, Du C, Dempsey CE, Hancox JC. High potency inhibition of hERG potassium channels by the sodium-calcium exchange inhibitor KB-R7943. Br J Pharmacol. 2012;165(7):2260–73.

37. Braga RC, Alves VM, Silva MFB, Muratov E, Fourches D, Lião LM, et al. Pred-hERG: A Novel web-Accessible Computational Tool for Predicting Cardiac Toxicity. Mol Inform. 2015;34(10):698–701.

38. Alves VM, Muratov E, Fourches D, Strickland J, Kleinstreuer N, Andrade CH, et al. Predicting chemically-induced skin reactions. Part II: QSAR models of skin permeability and the relationships between skin permeability and skin sensitization. Toxicol Appl Pharmacol [Internet]. 2015;284(2):273–80. Available from: http://dx.doi.org/10.1016/j.taap.2014.12.013

39. Mali SN, Pandey A, Thorat BR, Lai C-H. Greener Synthesis, In-Silico and Theoretical Analysis of Hydrazides as Potential Antituberculosis Agents (Part 1). 2022;(Part 1):86.

40. Anuse, D.G.; Mali, S.N.; Thorat, B.R.; Yamgar, R.S.; Chaudhari, H.K. Synthesis, SAR, In-silico appraisal and Anti-Microbial Study of substituted 2-aminobenzothiazole derivatives. Curr Comput Aided Drug Des, 2019,15,1. http://dx.doi.org/10.2174/1573409915666191210125647 [PMID: 31820704]

41. Thorat, B.R.; Rani, D.; Yamgar, R.S.; Mali, S.N. Synthesis, In-silico and In-vitro analysis of hydrazones as potential anti-tuberculosis agents. *Curr comput Aided Drug Des*, 2020.

42. Thorat, B.R.; Rani, D.; Yamgar, R.S.; Mali, S.N. Synthesis, In-silico and In-vitro and computational analysis of hydrazones as potential anti-tuberculosis agents. *Curr comput Aided Drug Des*; 2021.